www.nature.com/aps

Acta Pharmacologica Sinica

ARTICLE

Sapidolide A alleviates acetaminophen-induced acute liver injury by inhibiting NLRP3 inflammasome activation in macrophages

Jin-cheng Wang[1], Qi Shi[1,2], Qian Zhou[3], Lu-lu Zhang[1], Yue-ping Qiu[1], Da-yong Lou[4], Li-qin Zhou[4], Bo Yang[1,2], Qiao-jun He[1,2], Qin-jie Weng[1,2] and Jia-jia Wang[1]

Macrophages play a critical role in the pathogenesis of acetaminophen (APAP)-induced liver injury (AILI), a major cause of acute liver failure or even death. Sapidolide A (SA) is a sesquiterpene lactone extracted from *Baccaurea ramiflora* Lour., a folk medicine used in China to treat inflammatory diseases. In this study, we investigated whether SA exerted protective effects on macrophages, thus alleviated the secondary hepatocyte damage in an AILI. We showed that SA (5–20 μM) suppressed the phosphorylated activation of NF-κB in a dose-dependent manner, thereby inhibiting the expression and activation of the NOD-like receptor protein 3 (NLRP3) inflammasome and pyroptosis in LPS/ATP-treated mouse bone marrow-derived primary macrophages (BMDMs). In human hepatic cell line L02 co-cultured with BMDMs, SA (10 μM) protected macrophages from the pyroptosis induced by APAP-damaged L02 cells. Moreover, SA treatment reduced the secondary liver cell damage aggravated by the conditioned medium (CM) taken from LPS/ATP-treated macrophages. The in vivo assessments conducted on mice pretreated with SA (25, 50 mg/kg, ip) then with a single dose of APAP (400 mg/kg, ip) showed that SA significantly alleviated inflammatory responses of AILI by inhibiting the expression and activation of the NLRP3 inflammasome. In general, the results reported herein revealed that SA exerts anti-inflammatory effects by regulating NLRP3 inflammasome activation in macrophages, which suggests that SA has great a potential for use in the treatment of AILI patients.

Keywords: acetaminophen; acute liver injury; Sapidolide A; bone marrow-derived primary macrophages (BMDM); pyroptosis; NLRP3 inflammasome

Acta Pharmacologica Sinica (2022) 43:2016–2025; https://doi.org/10.1038/s41401-021-00842-x

INTRODUCTION

Drug-induced liver injury is a growing medical problem worldwide [1, 2], and more than 40%–50% of cases are caused by accidental or intentional (suicidal) intake of high doses of acetaminophen (APAP) [3]. APAP-induced liver injury (AILI) is developed via two pathological stages: APAP-induced direct cellular damage and sterile inflammation-mediated disease progression [4, 5]. First, APAP undergoes catalytic degradation by a P450 cytochrome, mainly CYP2E1, to form a reactive metabolite, *N*-acetyl-*p*-benzoquinoneimine (NAPQI), that causes glutathione depletion and mitochondrial dysfunction in hepatocytes [5]. The dysfunctional mitochondria lead to cellular ATP depletion, DNA fragmentation and cell necrosis [5]. Meanwhile, the necrotic hepatocytes can release damage-associated molecular patterns (DAMPs), resulting in the abnormal activation of the innate immune system, which further contributes to the development of AILI [6, 7]. So far, *N*-acetyl cysteine (NAC) is the only agent for AILI treatment approved by the Food and Drug Administration [8], and since it works mainly by detoxifying NAPQI in the initial stage, this treatment is only effective if administered within 8 h of APAP ingestion [9, 10]. Therefore, the development of alternative treatments that target the second stage of AILI is of great importance.

Liver macrophages, including resident Kupffer cells (KCs) and infiltrated monocyte-derived macrophages (MoMFs), play major roles in the pathogenesis of AILI [11, 12]. Specifically, DAMPs recruit and activate macrophages to release various pro-inflammatory cytokines and chemokines, thereby promoting immune cell infiltration and enhancing immune response [13–15]. However, the activated macrophages may also act as phagocytes that remove necrotic cell debris, which promotes liver regeneration in AILI [16, 17]. These contrasting roles of macrophages mainly depend on whether they are polarized towards pro-inflammatory M1 or anti-inflammatory M2 phenotypes in response to multiple stimuli [18]. M1 macrophages produce pro-inflammatory cytokines and chemokines that contribute to the development of AILI, while M2 macrophages release anti-inflammatory cytokines and are involved in the phagocytosis of dying cells [19]. Therefore, the

[1]Center for Drug Safety Evaluation and Research, Zhejiang Province Key Laboratory of Anti-Cancer Drug Research, College of Pharmaceutical Sciences, Zhejiang University, Hangzhou 310058, China; [2]Hangzhou Institute of Innovative Medicine, College of Pharmaceutical Sciences, Zhejiang University, Hangzhou 310058, China; [3]Department of Pharmacy, Hangzhou Medical College, Hangzhou 310053, China and [4]Medication Department, Zhuji People's Hospital of Zhejiang Province, Zhuji, Shaoxing 311800, China
Correspondence: Jia-jia Wang (wangjiajia3301@zju.edu.cn)
These authors contributed equally: Jin-cheng Wang, Qi Shi, Qian Zhou

Received: 10 August 2021 Accepted: 10 December 2021
Published online: 12 January 2022

therapeutic strategies that rely on macrophage targeting have great potential for the treatment of AILI.

Interestingly, dysregulation of macrophage inflammasome activation and pyroptosis has been observed during AILI development, as reported in a recent study [20]. Pyroptosis is a newly identified inflammatory form of caspase-1-dependent cell death, with biochemical and morphological features of apoptosis and necrosis. This process is driven by NOD-like receptor protein 3 (NLRP3) inflammasome activation, one of the core mechanisms for innate immune defense, which induces the release of interleukin (IL)-1β and IL-18 pro-inflammatory cytokines [21, 22]. IL-1β is a powerful pro-inflammatory mediator whose levels increase during APAP hepatotoxicity, resulting in the activation and infiltration of leukocytes in the liver, which aggravates hepatocyte damage [23]. So far, different views have been held on the roles of NLRP3 and caspase-1 in AILI. Some studies suggested that NLRP3-mediated pyroptosis contributes to AILI and caspase-1 deficiency suppresses it [4, 20, 23]. Meanwhile, another study reported that the mild endogenous formation of IL-1β and NLRP3 deficiency have little impact on APAP hepatotoxicity [24, 25]. Although the relevance of pyroptosis in AILI remains controversial, many studies show that AILI may be alleviated by interfering with NLRP3 inflammasome activation [20, 26–28].

Baccaurea ramiflora Lour., a tall evergreen tree belonging to the Euphorbiaceae family, is widely distributed in the Karst region of southwest China [29]. Considering the analgesic, anti-inflammatory, and free radical scavenging effects of this tree, it has been used as a folk medicine in China to treat rheumatoid arthritis, cellulitis, apostema and injury from falls [30]. Rosmarinic acid is the only identified anti-inflammatory component in *Baccaurea ramiflora* Lour., and little is known about the single functional monomer [30]. Recently, a type of sesquiterpene lactone called Sapidolide A (SA) has been isolated from the berries of *B.ramiflora* and exhibits antifungal activity [31]. The anti-inflammatory activity of this compound is yet to be explored.

In this study, we show that SA significantly inhibits the expression and activation of the NLRP3 inflammasome and suppresses pyroptosis in macrophages, without affecting macrophage polarization. Then, SA can protect macrophages from pyroptosis caused by APAP-damaged liver cells, and SA-treated macrophages reduce the secondary death of liver cells. Moreover, functional studies indicate that SA significantly improves AILI and blocks inflammation in vivo and it inhibits the activation of NLRP3 inflammasomes in AILI mice. Overall, our findings reveal for the first time that SA plays a role in inhibiting NLRP3 inflammasome activation in macrophages, thereby protecting liver cells from AILI. This suggests that SA can be used as an alternative approach or even a supplementary agent for the treatment of AILI patients.

MATERIALS AND METHODS

Animals and drug treatments

Male C57BL/6 mice (7–8 weeks old, specific pathogen-free) were purchased from Beijing Vital River Laboratory Animal Technology Co., Ltd. All mice were maintained in specific pathogen-free and temperature-controlled individual ventilated cages with a 12-h light and dark cycle. All animal use and studies were performed in compliance with all relevant ethical regulations and were approved by the Institutional Animal Care and Use Committee at Zhejiang University.

After fasting for 14 h, mice received a single intraperitoneal injection with APAP (400 mg/kg, Aladdin) dissolved in warm sterile saline. SA (purity > 99%) was kindly gifted from Professor Lishe Gan. Mice were pretreated with SA (25, 50 mg/kg, dissolved in saline) by intraperitoneal injection 1 h before APAP challenge. Control mice were treated with an injection of vehicle (normal saline). Standard chow and wet mash were returned to mice 2 h post-APAP administration. The mice were sacrificed 6 or 24 h after normal saline or APAP injection, and serum and liver tissues were collected and stored at −80 °C for further analysis.

Cell culture

Bone marrow-derived primary macrophages (BMDMs) were generated by culturing bone marrow cells isolated from femurs and tibias of C57BL/6 mice in DMEM (Gibco, ThermoFisher) containing 10% fetal bovine serum (Gibco) plus macrophage colony-stimulating factor (M-CSF, 50 ng/ml, Peprotech) for 7 d. Human hepatic cell line L02 cells were purchased from Shanghai Institute of Biochemistry and Cell Biology (Shanghai, China), cultured in RPMI- 1640 (Gibco, ThermoFisher) containing 10% fetal bovine serum (Gibco).

Cell viability assay

Cell viability was measured by sulforhodamine B (SRB) assay. Briefly, 100 μL cold trichloroacetic acid (10%) was added into each well to fix the adherent cells and the plates were incubated at 4 °C for 1 h. The plates were then washed five times with deionized water and dried in the air. Each well was then added with 50 μL SRB solution (0.4% *w/v* in 1% acetic acid) and incubated for 30 min at room temperature. The plates were washed five times with 1% acetic acid to remove the unbound SRB completely and then dried in the air. The residual bound SRB was solubilized with 100 μL of 10 mM Tris base buffer. The absorbance was measured at 495 nm on a multiscan spectrum (Thermo Multiskan Spectrum, Thermo Electron Corporation, USA).

NLRP3 inflammasome activation assay and application of conditioned medium (CM)

BMDMs were stimulated with LPS (250 ng/mL, Sigma-Aldrich) for 4 h as the first signal for NLRP3 inflammasome action. Medium was replaced with serum-free medium and then the indicated doses of SA were added for 1 h. Cells were then stimulated with ATP (5 mM, MedChemExpress) for 1 h to activate the NLRP3 inflammasome. The CM from LPS/ATP-stimulated BMDMs with or without SA treatment (Ctrl-CM or SA-CM) were collected and centrifuged to remove the cell debris and then added to L02 cells at a ratio of 1 volume of CM: 1 volume of RPMI-1640 containing 10% fetal bovine serum [32].

Cell co-culture experiments

For transwell co-culture experiments, cells were performed in 24-well cultured plates with 8 μm pore size transwell chamber inserts (Falcon). L02 cells were seeded into the upper chambers and treated with APAP (10 mM) for 24 h. Then the L02 cells were co-cultured with BMDMs seeded into the bottom chambers and treated with SA (10 μM) for 24 h.

Western blotting

Cells were lysed in a RIPA buffer (50 mM Tris-HCl, pH 7.4, 1% NP-40, 0.25% sodium deoxycholate, 150 mM NaCl, 1 mM EGTA, 1 mM PMSF, 1 mM Na_3VO_4, 10 μg/mL aprotinin, 10 μg/mL leupeptin), and the supernatants were precipitated with methanol/chloroform, followed by centrifugation at 20,000 × *g* for 10 min. The upper phase was discarded, and one volume of methanol was added. The mixture was centrifuged at 20,000 × *g* for 10 min to obtain a protein pellet that was dried at room temperature and then resuspended in Laemmli buffer (0.25 M Tris-HCl, pH 6.8, 0.4% glycerol, 10% SDS, 0.2% 2-mercaptoethanol, 0.64% bromophenol blue). The protein samples were separated by 10% SDS-PAGE gels and transferred onto polyvinylidene difluoride membrane using a wet transfer system. Membranes were blocked in 5% (wt/vol) non-fat milk in T-PBS (20 mM Tris-HCl, pH 7.6, 150 mM NaCl, and 0.1% (vol/vol) Tween-20) for 1 h at room temperature. Membranes were incubated with primary antibody diluted in T-PBS at 4 °C overnight. After being washed with T-PBS, the membrane was incubated with the appropriate horseradish peroxidase-

conjugated secondary antibody diluted in 5% non-fat milk in T-PBS for 1 h at room temperature. The membranes were further developed with AI100. Primary antibodies used were as follows: anti-cleaved-caspase-1 (#89332), anti-IL-1β (#31202), anti-p-NF-κB p65 (#3033), anti-NF-κB p65 (#8242), anti-PARP (#9542) and anti-HMGB1 (#6893) were from Cell Signaling Technology; anti-pro-caspase-1 (ab179515) was from Abcam; anti-p-JNK (sc-6254) and anti-JNK (sc-7345) were from Santa Cruz; anti-GAPDH (db106) was from Diagbio. Secondary HRP-conjugated antibodies used were goat anti-mouse IgG (70-GAM0072), goat anti-rabbit IgG (70-GAR0072) (Multi Sciences).

Real-time quantitative PCR (qRT-PCR)
Total RNA was isolated from kidney tissues using Trizol reagent (Invitrogen, Carlsbad, California, USA) in accordance with the manufacturer's protocol, and cDNA was prepared using a cDNA preparation supermix (TransGen Biotech, Beijing, China). qRT-PCR was carried out using SYBR Green Supermix (Bio-Rad, Hercules, California, USA) with 20 μL reaction mixtures. PCR reactions were performed on the Quant Studio 6 Flex Real-Time PCR System (Applied Biosystems, Carlsbad, California, USA) with the following program: step 1, 95 °C for 3 min to activate the Taq polymerase; step 2, 95 °C for 3 s to denaturize DNA; step 3, 60 °C for 31 s for annealing/extension (39 cycles for steps 2 and 3). The relative mRNA levels were quantified by the $2^{-\Delta\Delta Ct}$ method and all data were normalized to GAPDH (the internal control).

Hematoxylin and eosin (H&E) staining
Liver tissues from the mice were fixed in 10% formalin, embedded in paraffin wax and cut into 3 μm-thick tissue sections. Sections of paraffin-embedded tissues were stained with H&E. H&E staining signals were quantified by NIH ImageJ software.

Blood biochemical analysis for liver function
Serum alanine aminotransferase (ALT) and aspartate aminotransferase (AST) levels were measured by the Infinity ALT Kit (Thermo Scientific) and AST Kit (Bioo Scientific), respectively.

Enzyme-linked immunosorbent assay (ELISA)
The IL-18 and IL-1β levels in culture media and serum were determined using a DuoSet ELISA kit (eBioscience Technology, Shenzhen, China) according to the manufacturer's protocols.

Immunostaining analysis
Liver cryosections (8 μm) were incubated with a blocking buffer (PBS with 5% normal goat serum and 0.3% Triton-100) for 1 h. Terminal deoxynucleotidyl transferase dUTP nick-end labeling (TUNEL) staining was conducted as protocol (Beyotime). Apoptosis-associated speck-like protein containing a CARD (ASC) staining was performed with rabbit anti-ASC (Adipogen, AG-25B-0006), CD68 staining was performed with rabbit anti-CD68 (Santa Cruz, sc-20060). The secondary antibodies were as follows: anti-rabbit secondary antibody (Beijing Zhongshan Biotechnology, PV-6001), Alexa Fluor® 488 anti-rabbit IgG secondary antibody (Invitrogen, A-11008), with DAPI (4′,6-diamidino-2-phenylindole, dihydrochloride; Vector Laboratories) for nuclear counterstaining. Images were acquired using an Olympus BX51 system microscope equipped with SPOT camera and SPOT Advanced 5.1 software. TUNEL, ASC, CD68 staining signals were quantified by NIH Image J software. Specifically, ASC specks were counted in five random areas of each image in triplicate experiments, and a minimum of 100 cells from each treatment condition were quantified.

Nonparenchymal cell isolation and flow cytometry
Livers from mice were digested by collagenase type IV (Gibco), and intrahepatic leukocytes were isolated by multiple differential centrifugation steps. Then the cells were incubated for 30 min at 4 °C with 3% BSA, and then stained with the following antibodies: CD45 (PerCP-Cy5.5, Biolegend, 5300727), CD11b (FITC, Biolegend, 5274805), F4/80 (PE/Cy7, Biolegend, 123114), Gr-1 (FITC, Biolegend, 108405). After staining, all cells were subjected to red cell lysis by home-made Split red liquid (8.29 g NH_4Cl, 1 g KHCO3, 37.2 mg EDTA 2Na, dissolved in 1 L deionized water, pH = 7.2) before analyzing in a BD FACS-Calibur cytometer (Becton Dickinson, San Jose, CA).

Co-immunoprecipitation (Co-IP)
For Co-IP of endogenous interaction between NLRP3 and ASC/Caspase 1, BMDMs were stimulated with LPS (250 ng/mL) for 4 h. After that, SA (10 μM) or CY-09 (10 μM, TopScience, USA, T4164) was added into the culture for another 30 min, and then the cells were stimulated with ATP (5 mM) for 1 h. Cells were lysed in a RIPA buffer and whole cell lysates were incubated with NLRP3 (Adipogen, AG-20B-0014-C100) or control IgG (Santa Cruz), followed by IP using Protein A/G magnetic beads (Bimake, B23201) and detection of ASC and pro-caspase-1 using specific antibodies.

Statistical analysis
Statistical analysis was performed using Image J (version 1.8.0) and GraphPad Prism Software (Version 8.0.1). Unpaired two-tailed Student's *t*-test or one-way ANOVA Tukey's *post-hoc* analysis was performed to determine statistical significance between two samples or for multiple comparisons, respectively. All data were from at least three independent experiments and presented as means ± SD. A value of $P < 0.05$ was considered statistically significant (represented as $^{*}P < 0.05$, $^{**}P < 0.01$, $^{***}P < 0.001$, or not significant (n.s.)).

RESULTS

SA prevents cell pyroptosis in macrophages
To understand whether SA affects the activation of macrophages in response to proinflammatory stimuli, mouse BMDMs were treated with this compound. It was confirmed that SA was not toxic to macrophages (Fig. 1a, b). Using LPS (250 ng/mL) and ATP (5 mM) stimulation in BMDMs, the NLRP3-inflammasome-activation-driven cell pyroptosis model was established, and analysis of these cells indicated that SA treatment increased cell viability in a concentration-dependent manner (Fig. 1c). In addition, SA treatment blocked the expression of pyroptosis markers, the cleavage of caspase-1 (cleaved-CASP-1), and the degradation of pro-IL-1β to mature IL-1β (cleaved-IL-1β) (Fig. 1d, e). Overall, these data suggested that SA can inhibit the macrophage pyroptosis induced by NLRP3 inflammasome activation.

Given that macrophage polarization plays a key role in immune response, the effect of SA treatment on the polarization of macrophages was also investigated. For this purpose, LPS-induced M1-polarized BMDMs and IL-4-induced M2-polarized BMDMs were treated with SA, and the levels of macrophage polarization markers in these cells were detected. The administration of SA did not alter the mRNA levels of M1 (*Il6* and *Inos*) and M2 markers (*Mrc1* and *Arg1*) in polarized BMDMs (supplementary Fig. 1a, b), which suggested that this compound has no effect on macrophage polarization.

SA suppresses the expression and activation of the NLRP3 inflammasome in macrophages
The NLRP3 inflammasome is canonically activated via two parallel and independent steps: priming (transcription) and activation (oligomerization) [33, 34]. LPS stimulation first induces the activation of nuclear factor κB (NF-κB) signaling. Then, the active NF-κB primes the NLRP3 inflammasome for activation by promoting the transcription of NF-κB-dependent genes, such as *Nlrp3*, *Il1β*, and *Il18* [35–38]. To assess the effect of SA on the

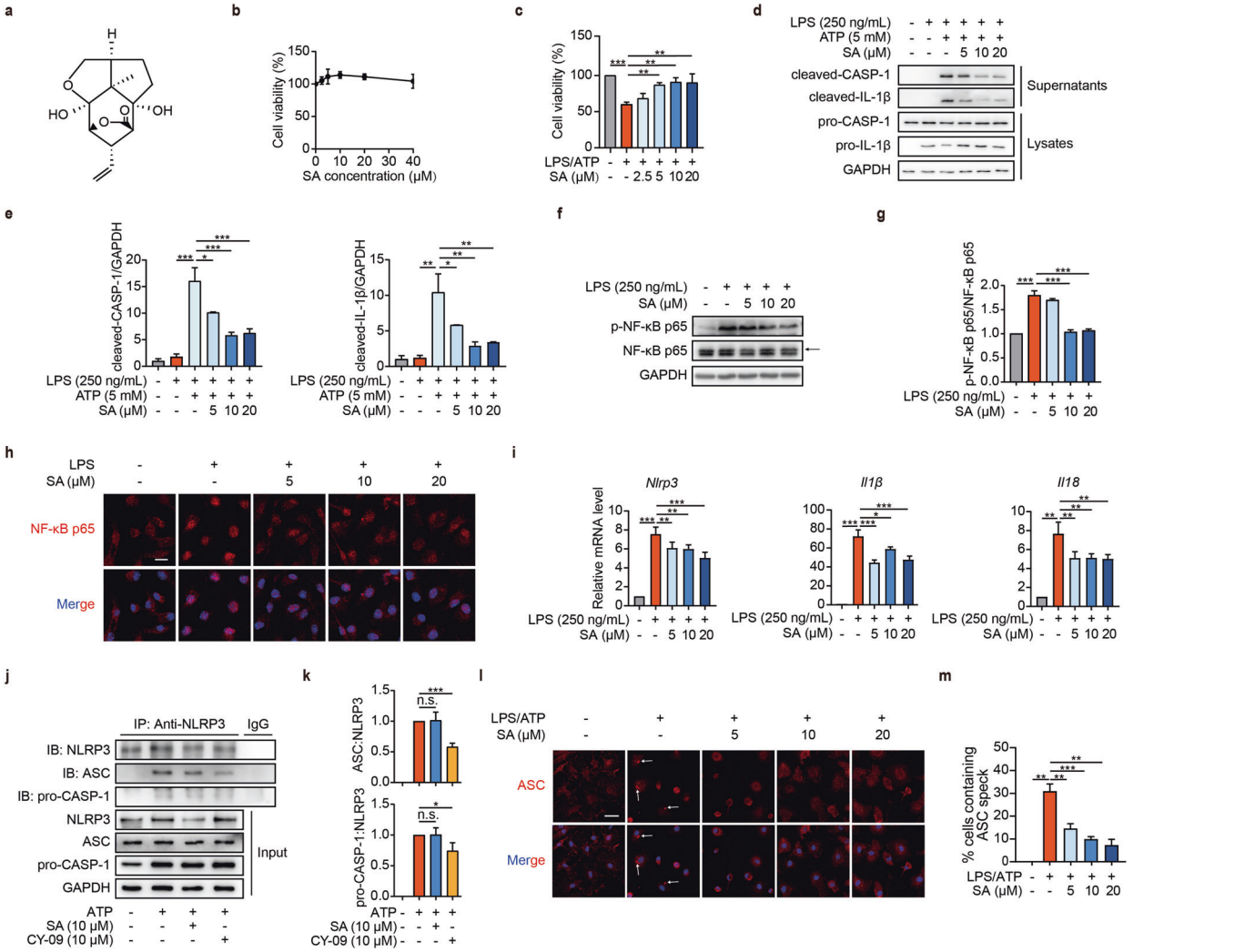

Fig. 1 SA inhibits NLRP3 inflammasome-mediated pyroptosis in macrophages. a Chemical structure of SA. **b** BMDMs were treated with SA (0.625, 1.25, 2.5, 5, 10, 20, 40 μM) for 24 h. SRB assay for cell viability. **c** BMDMs were primed with LPS (250 ng/mL) for 4 h. The cells were treated with or without SA for 1 h and then stimulated with ATP (5 mM) for 1 h. SRB assay for cell viability. **d**, **e** BMDMs were primed with LPS (250 ng/mL) for 4 h. Medium was replaced with serum-free medium and then the indicated doses of SA were added for 1 h, and then stimulated with ATP (5 mM) for 1 h. Western blotting for expression of pro-caspase-1 (pro-CASP-1) and pro-IL-1β in cell lysates, and cleaved-CASP-1 and cleaved-IL-1β in cell supernatants. Relative protein levels compared with GAPDH were shown as line graphs. **f**, **g** BMDMs were pre-treated with SA for 1 h and then stimulated with LPS (250 ng/mL) for 4 h. Western blotting for expression of (p)-NF-κB p65 in cell lysates. Relative p-NF-κB p65 level compared with NF-κB p65 was shown as a line graph. **h** Immunostaining of NF-κB p65 (red) and DAPI (blue) in BMDMs. Scale bar: 10 μm. **i** qRT-PCR assays for *Nlrp3*, *Il1β* and *Il18* in cell lysates of BMDMs. **j**, **k** Co-IP and Western blotting for the interaction of endogenous NLRP3 and ASC in LPS-primed BMDMs treated with SA (10 μM) or CY-09 (10 μM) and then stimulated with ATP (5 mM). **l**, **m** BMDMs were primed with LPS (250 ng/mL) for 4 h. The cells were treated with or without SA for 1 h and then stimulated with ATP (5 mM) for 1 h. Immunostaining of ASC (red) and DAPI (blue) in BMDMs. The arrows indicate ASC specks. Scale bar: 25 μm. Quantification of ASC-positive cells/total cells by Image J software. $n = 3$ independent experiments. Data are presented as means ± SD. $^{*}P < 0.05$, $^{**}P < 0.01$, $^{***}P < 0.001$; n.s. no significance.

expression and activation of NLRP3 inflammasome, the levels of active NF-κB p65 (p-NF-κB p65) in LPS-stimulated BMDM lysates were assessed by Western blotting in the presence or absence of SA. The results indicated that SA decreased the phosphorylation of NF-κB p65 in macrophages (Fig. 1f, g) and blocked the LPS-induced transport of NF-κB p65 into the nucleus to regulate transcription (Fig. 1h). Therefore, in SA-treated macrophages, NF-κB p65 was retained in the cytoplasm (Fig. 1h). The qRT-PCR results demonstrated that, as expected, the mRNA levels of *Nlrp3*, *Il1β*, and *Il18* were downregulated by SA treatment (Fig. 1i). This implied that SA can suppress the expression and activation of the NLRP3 inflammasome in macrophages by inhibiting the first signal in the initial stage.

The second signal is NLRP3 activation and inflammasome assembly, which can be initiated by an array of DAMPs. Stimulation with an NLRP3 agonist, such as ATP, activates NLRP3 oligomerization and recruits pro-caspase-1 via the ASC adapter [33, 34]. Therefore, ASC speck formation is a prerequisite for pro-caspase-1 degradation and auto-activation [39]. To examine whether SA can interfere with NLRP3 inflammasome assembly, endogenous Co-IP assays were performed on NLRP3-inflammasome-activated BMDMs. The obtained results showed that SA did not affect the interaction between NLRP3 and ASC/caspase-1; however, the direct NLRP3 inhibitor CY-09 suppressed NLRP3/ASC/caspase-1 interaction in LPS/ATP-primed BMDMs (Fig. 1j, k). Therefore, it may be concluded that SA does not affect the second signal of inflammasome activation. Instead, it reduced ATP-induced formation of ASC specks in BMDMs (Fig. 1l, m), resulting in decreased levels of active caspase-1 (cleaved-CASP-1) (Fig. 1d, e). The active caspase-1 then cleaves pro-IL-1β and pro-IL-

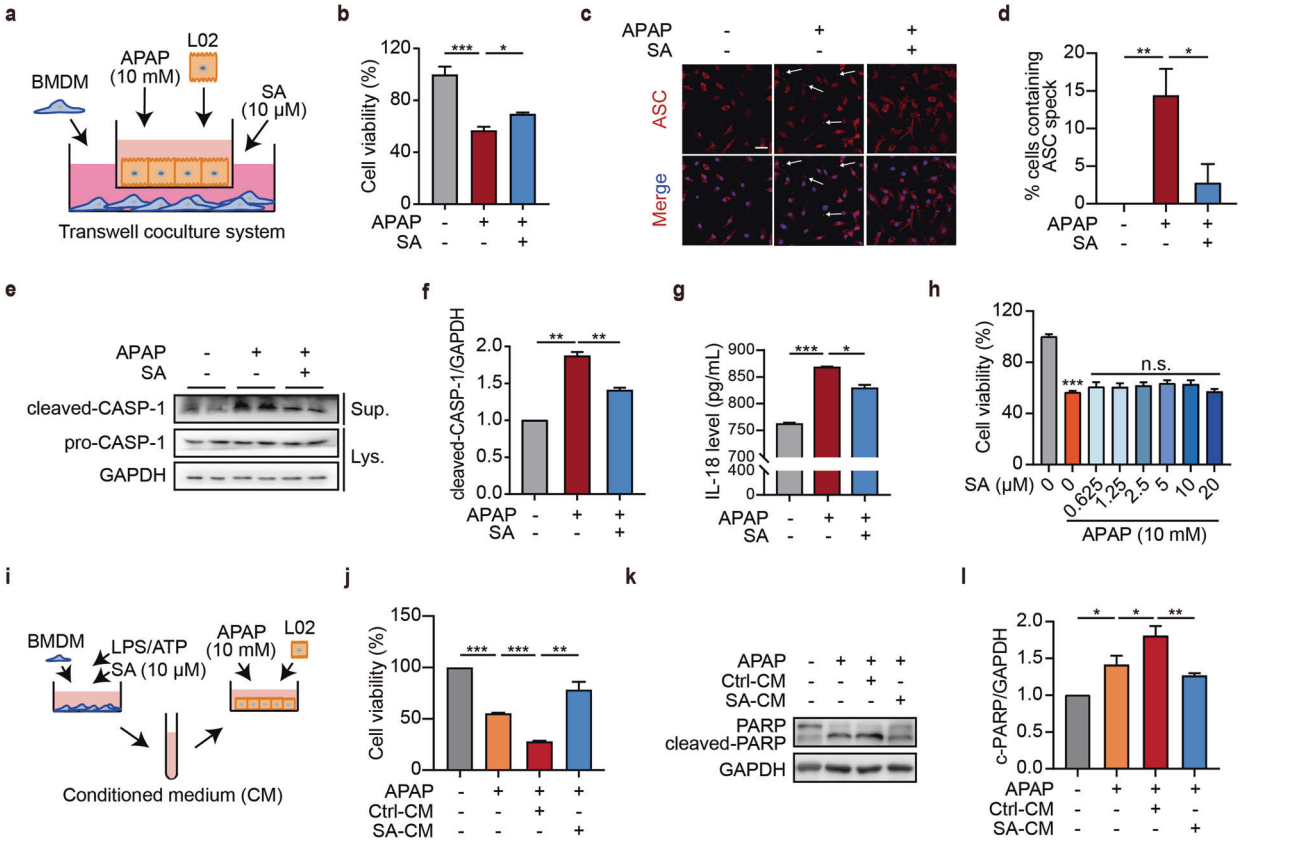

Fig. 2 SA suppresses APAP-induced NLRP3 inflammasome activation in macrophages, which promotes hepatocyte damage. a Experimental scheme of SA and APAP treating strategy in BMDM and L02 cells. L02 cells were seeded into the upper chambers and treated with APAP (10 mM) for 24 h. Then the L02 cells were co-cultured with BMDMs seeded into the bottom chambers and treated with SA (10 μM) for 24 h. **b** SRB assay for viability of BMDMs. **c**, **d** Immunostaining of ASC (red) and DAPI (blue) in BMDMs. The arrows indicate ASC specks. Scale bar: 25 μm. Quantification of ASC-positive cells/total cells by Image J software. **e**, **f** Western blotting for expression of pro-caspase-1 (pro-CASP-1) in cell lysates, and cleaved-CASP-1 in cell supernatants. Relative cleaved-CASP-1 level compared with GAPDH was shown as a line graph. **g** Levels of IL-18 in cell supernatants were detected by ELISA. **h** L02 cells were treated with APAP (10 mM) with or without SA (0.625, 1.25, 2.5, 5, 10, 20 μM) for 24 h. SRB assay for cell viability. **i** Experimental scheme of SA and APAP treating strategy in BMDMs and L02 cells. L02 cells were cultured with Ctrl-CM or SA-CM of BMDMs with an additional APAP (10 mM) for 24 h. **j** SRB assay for viability of L02 cells. **k**, **l** Western blotting for expression of (cleaved)-PARP in L02 cells. Relative cleaved-PARP level compared with GAPDH was shown as a line graph. $n = 3$ independent experiments. Data are presented as means ± SD. $^*P < 0.05$, $^{**}P < 0.01$, $^{***}P < 0.001$; n.s. no significance.

18 into their mature forms, leading to the secretion of these cytokines [40, 41]. Mature IL-1β and IL-18 are thus considered hallmarks of NLRP3 inflammasome activation, and the results showed that they were blocked by SA treatment (Fig. 1d, e). In general, the results obtained herein suggested that SA suppresses the expression and activation of the NLRP3 inflammasome in macrophages by inhibiting NF-κB signaling.

SA inhibits damaged hepatocyte-induced NLRP3 inflammasome activation in macrophages

Considering that APAP-induced liver injury involves severe immune response, such as NLRP3 inflammasome activation, the impact of SA on AILI-stimulated inflammasome activation was also evaluated. To mimic the direct effect of APAP-damaged hepatocytes on macrophages, a transwell coculture system of BMDMs and human hepatic cell line L02 was set up (Fig. 2a). The BMDMs cocultured with APAP-damaged L02 cells exhibited massive death (Fig. 2b). However, SA treatment increased the viability of BMDMs compared to the control cells, which indicated that SA reduced the rate of macrophage death caused by damaged hepatocytes (Fig. 2b). Based on the immunostaining results, SA treatment also suppressed the formation of ASC specks in BMDMs by APAP-damaged L02 cells (Fig. 2c, d). In addition, the Western blots of SA-treated BMDMs supernatants demonstrated that SA decreased the expression of cleaved-caspase-1 (Fig. 2e, f). As expected, the levels of IL-18 in SA-treated BMDM supernatants were lower than those detected in the control group (Fig. 2g). Together, these data suggested that SA inhibits APAP-damaged hepatocyte-induced NLRP3 inflammasome activation in macrophages.

SA inhibits NLRP3 inflammasome activation in macrophages to alleviate secondary hepatocyte damage

Given that the expansion of inflammation in AILI aggravates the secondary damage of hepatocytes, we next investigated whether SA-induced macrophage pyroptosis reduction could relieve this damage. First, the influence of SA on the survival rate of APAP-stimulated L02 cells was assessed (Fig. 2h). Then, BMDMs were treated with LPS/ATP to induce NLRP3 inflammasome activation. The conditioned medium (CM) of macrophage pyroptosis in the induced cells was subsequently collected, with or without SA treatment. The collected CM was primed and added to L02 cells, along with APAP, to investigate its effect on hepatocyte survival after 24 h of exposure (Fig. 2i). Based on the SRB assay results, Ctrl-CM severely aggravated the death of APAP-induced L02 cells; however, SA-CM significantly increased the viability of these cells (Fig. 2j). Similar results were also observed for the expression of cleaved-PARP in L02 cells treated with CM (Fig. 2k, l). Overall, these results suggested that SA treatment protects hepatocytes against APAP-induced damage by inhibiting the activation of the NLRP3 inflammasome in macrophages.

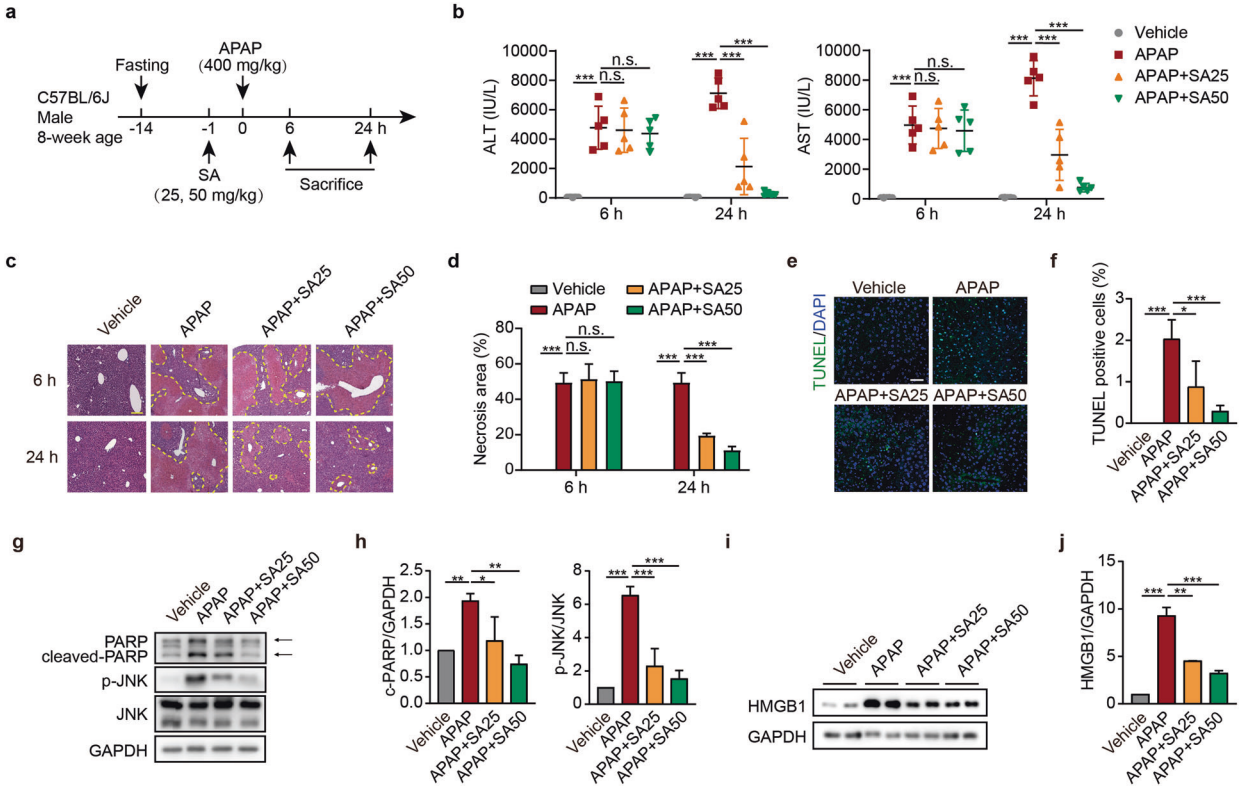

Fig. 3 SA protects against APAP-induced acute liver injury. a Experimental scheme of SA and APAP treating strategy in mice. The mice were treated with saline (intraperitoneal injection, i.p.) or SA (i.p., 25 or 50 mg/kg) 1 h before APAP (i.p., 400 mg/kg) administration and the mice were sacrificed at 6 or 24 h after APAP. **b** Serum ALT and AST levels of AILI mice treated with APAP with or without SA. **c**, **d** Representative H&E staining of liver sections from AILI mice treated with APAP with or without SA. Scale bar: 200 μm. Quantification of necrotic areas by Image J software. **e**, **f** Representative TUNEL assay of liver sections from AILI mice treated with APAP 24 h with or without SA. Scale bar: 100 μm. Quantification of TUNEL-positive cells by Image J software. **g**, **h** Western blotting for expression of (cleaved)-PARP and (p)-JNK of liver tissues from AILI mice treated with APAP 24 h with or without SA. Relative cleaved-PARP level compared with GAPDH and p-JNK level compared with JNK were shown as line graphs. **i**, **j** Western blotting for expression of HMGB1 of liver tissues from AILI mice treated with APAP 24 h with or without SA. Relative HMGB1 level compared with GAPDH was shown as a line graph. $n = 5$ animals per group. Data are presented as means ± SD. $^{*}P < 0.05$, $^{**}P < 0.01$, $^{***}P < 0.001$.

SA protects against APAP-induced acute liver injury

To assess the potential protective function of SA against APAP-induced hepatotoxicity in vivo, an AILI mouse model was pre-treated with different doses of SA (25 and 50 mg/kg). Blood samples and liver tissues were collected from the treated mice at different time intervals (Fig. 3a). Biochemistry and histopathology analyses of these samples and tissues showed that without SA treatment, the mice suffering from AILI exhibited severe liver damage, as evidenced by their significantly elevated ALT and AST plasma levels after 6 and 24 h of APAP administration (Fig. 3b). Pre-treatment with SA substantially lowered the high concentrations of ALT and AST in AILI mice at 24 h, but not at 6 h (Fig. 3b). The H&E staining results demonstrated that the hepatocytes of AILI mice exhibited obvious cell ballooning, degeneration, and necrosis at 6 and 24 h; however, SA pre-treatment dramatically reduced the necrosis area at 24 h (Fig. 3c, d). In general, the obtained results indicated that SA can prevent liver injury at an advanced stage rather than at an early stage. This suggested that SA alleviates AILI by regulating the immune response instead of by directly interfering with APAP metabolism.

The TUNEL staining analyses of cell apoptosis and the Western blot analyses of cleaved-PARP performed after 24 h of APAP treatment showed that this treatment promoted the phosphorylation of c-Jun kinase (JNK) (Fig. 3e–h), which is correlated with liver injury [42, 43]. SA limited APAP-induced JNK phosphorylation, as determined by the Western blots of whole liver homogenates from SA-treated mice (Fig. 3g, h). In AILI, the death of hepatocytes triggered the release of DAMPs, such as high mobility group box-1 (HMGB1), a key injury mediator in APAP-induced liver toxicity [44–46]. The released DAMPs activate the production of pro-inflammatory cytokines by immune cells, thereby initiating immune response and aggravating hepatocyte damage [6, 47]. The Western blots demonstrated that SA reduced HMGB1 expression in AILI mice (Fig. 3i, j). Overall, the results suggested that SA attenuates APAP-induced hepatotoxicity.

Macrophage response is inhibited in SA-treated AILI mice

Macrophages are the initial and core immune cells that mediate inflammation in AILI [48–51]. Once activated by DAMP recognition, these cells release different types of pro-inflammatory cytokines and chemokines, thereby increasing the flux of immune cells (e.g., bone marrow-derived monocytes and neutrophils) and enhancing inflammation [6, 47]. To examine the effect of SA treatment on the immune response in AILI mouse livers, immunohistochemistry analysis of the CD68 macrophage marker was performed. The obtained results showed that SA reduced the number of CD68 positive cells in the livers of AILI mice (Fig. 4a, b), which suggested that this compound is capable of blocking the flux of macrophage. Cytometric analysis of KCs and infiltrated MoMFs, the main liver macrophages in the AILI model, revealed that AILI increased the number of MoMFs (identified as $CD11b^{int}F4/80^{low}$ cells) and decreased the number of KCs (identified as $CD11b^{low}F4/80^{hi}$ cells) within the $CD45^{+}$ liver cell population (Fig. 4c, d). SA treatment countered the effect of AILI

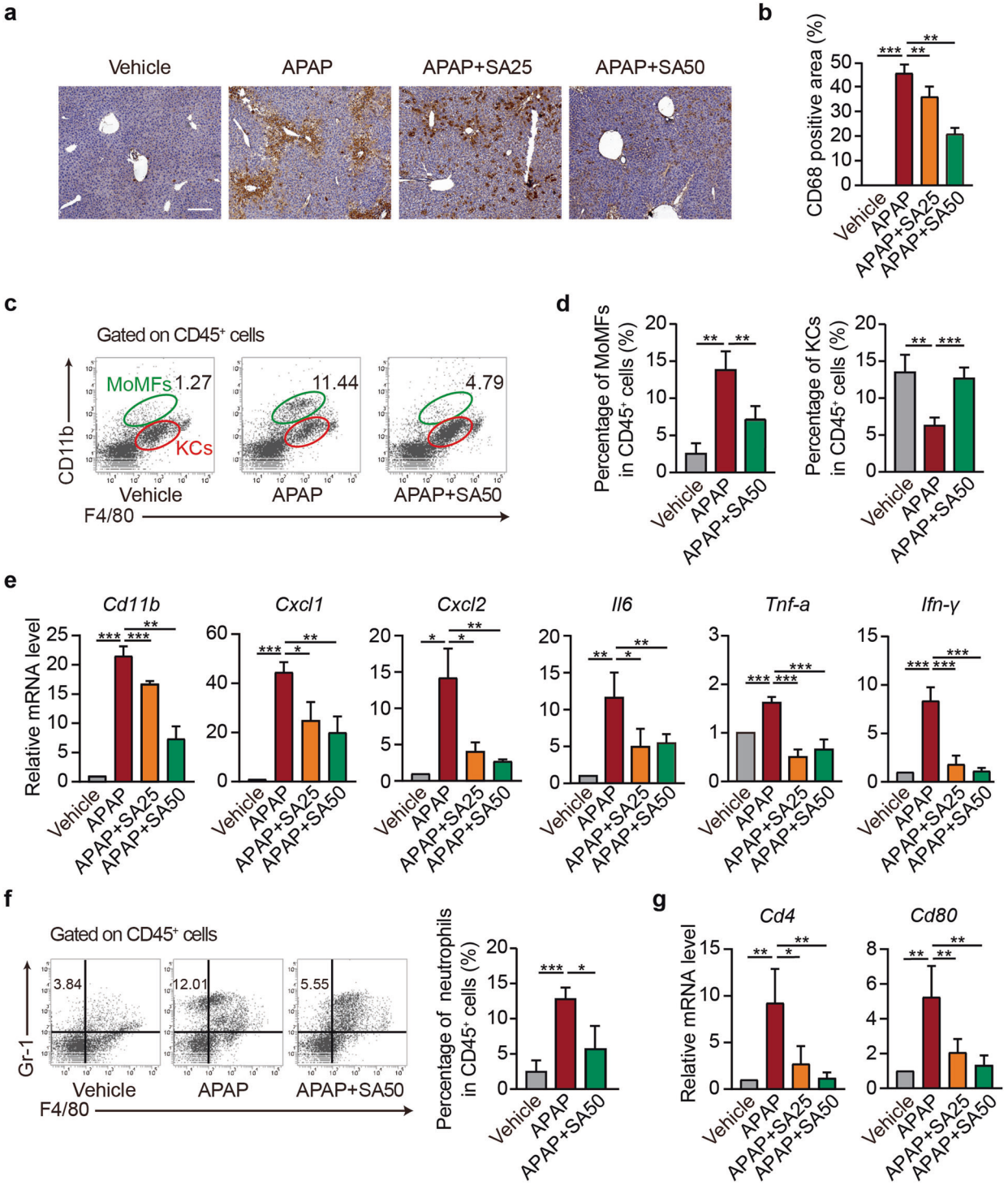

Fig. 4 SA reduces APAP-induced immune response. a, **b** Representative immunohistochemistry assay of CD68 in liver sections from AILI mice treated with APAP with or without SA. Scale bar: 100 μm. Quantification of CD68-positive area/total area by Image J software. **c**, **d** Flow cytometry analysis of MoMFs ($CD11b^{int}$ $F4/80^{low}$) and KCs ($CD11b^{low}$ $F4/80^{hi}$) in liver tissues from AILI mice treated with APAP with or without SA. Quantification of the percentage of MoMFs or KCs in $CD45^+$ cells. **e** qRT-PCR assays for *Cd11b*, *Cxcl1*, *Cxcl2*, *Il6*, *Tnf-a* and *Ifn-γ* in liver tissues from AILI mice treated with APAP with or without SA. **f** Flow cytometry for the number of neutrophils ($Gr\text{-}1^{hi}$ $F4/80^-$) in liver tissues from AILI mice treated with APAP with or without SA. **g** qRT-PCR assays for *Cd4* and *Cd80* in liver tissues from AILI mice treated with APAP with or without SA. $n = 5$ animals per group. Data are presented as means ± SD. $^*P < 0.05$, $^{**}P < 0.01$, $^{***}P < 0.001$.

by reducing the population of MoMFs and increasing the population of KCs (Fig. 4c, d). Moreover, SA-treated AILI mice exhibited significantly downregulated mRNA levels of the *Cd11b* macrophage marker, the *Cxcl1* and *Cxcl2* macrophage-related chemokines, and the *Il6, Tnf-a,* and *Ifn-γ* pro-inflammatory cytokines (Fig. 4e). SA treatment also decreased the population of recruited neutrophils ($Gr\text{-}1^{hi}F4/80^-$), $CD4^+$ T cells and $CD80^+$ dendritic cells in AILI mouse livers (Fig. 4f, g). Based on the obtained results, SA treatment relieves inflammation and blocks macrophage response in AILI mice.

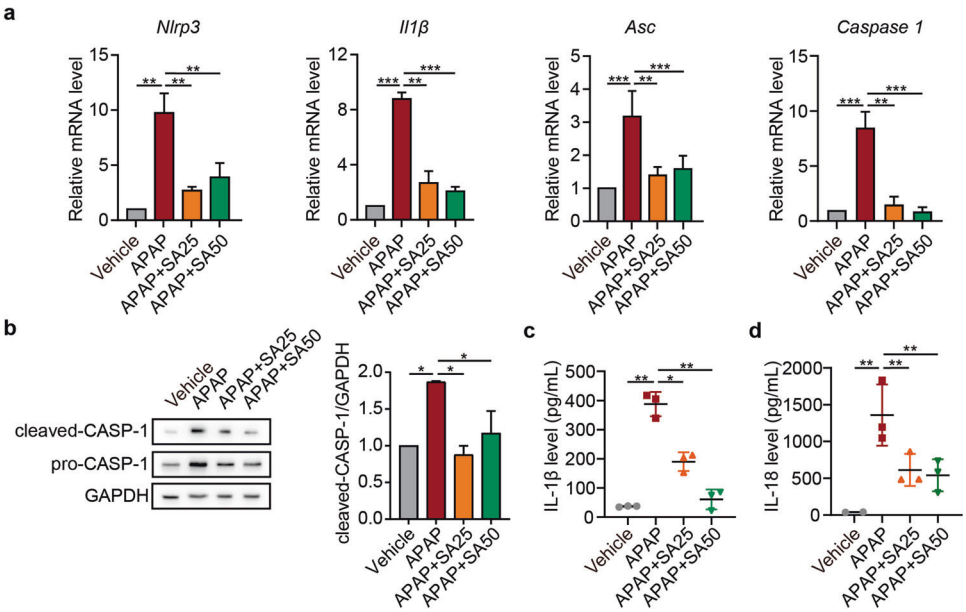

Fig. 5 SA suppresses NLRP3 inflammasome activation in AILI mice. The mice were treated with saline (intraperitoneal injection, i.p.) or SA (i.p., 25 or 50 mg/kg) 1 h before the administration of APAP (i.p., 400 mg/kg) and the mice were sacrificed at 24 h after APAP. **a** qRT-PCR assays for *Nlrp3*, *Il1β*, *Asc,* and *Caspase 1* in liver tissues from AILI mice treated with APAP with or without SA. **b** Western blotting for expression of pro-caspase-1 (pro-CASP-1) and cleaved-CASP-1 of liver tissues from AILI mice treated with APAP with or without SA. Relative cleaved-CASP-1 level compared with GAPDH was shown as a line graph. **c**, **d** Serum levels of IL-1β and IL-18 were detected by ELISA. $n = 3$ animals per group. Data are presented as means ± SD. $^{*}P < 0.05$, $^{**}P < 0.01$, $^{***}P < 0.001$.

SA suppresses NLRP3 inflammasome activation in AILI mice

The effect of SA on NLRP3 inflammasome activation in the AILI mouse model was also investigated. The results indicated that pre-treatment with SA lowered the expression of genes associated with the NLRP3 inflammasome, including *Nlrp3*, *Il1β*, *Asc* and *Caspase 1* (Fig. 5a). The reduced *Caspase 1* expression in SA-treated AILI mice was attributed to the inhibition of the IL-1/NF-κB pathway in hepatocytes [52]. SA obviously reduced the levels of cleaved-caspase-1 (Fig. 5b), and it also lowered the serum levels of IL-1β and IL-18 in AILI mice (Fig. 5c, d). These results confirmed that SA inhibits NLRP3 inflammasome activation in the AILI mouse model, resulting in decreased secretion of inflammatory factors such as IL-1β and IL-18.

DISCUSSION

Natural products play increasingly important roles in drug discovery and the treatment of many diseases and illnesses due to their numerous advantages, including few side effects, low toxicity, and high biological activity [53, 54]. However, the clinical application of these products is limited by insufficient compound quantities and the ambiguity of their precise mechanisms of action [55]. Moreover, rigorous clinical trials require the approval of different organizations [55]. Recently, numerous studies have demonstrated that the protective roles of natural products against AILI are related to multiple mechanisms, including anti-inflammation, antioxidation, and injury response mechanisms [56]. In this study, we investigated the anti-inflammatory activity SA, a sesquiterpenoid compound extracted from *Baccaurea ramiflora* Lour. This compound has previously been shown to exhibit antifungal activity [31]; however, to the best of our knowledge, its macrophage regulation function has not been reported before. In general, our results revealed that SA blocks the release of pro-inflammatory cytokines by inhibiting the expression and activation of the NLRP3 inflammasome in macrophages. This indicates that it can alleviate the secondary hepatocyte damage in AILI (Fig. 6), and thus, it has great potential as a supplementary agent for AILI treatment.

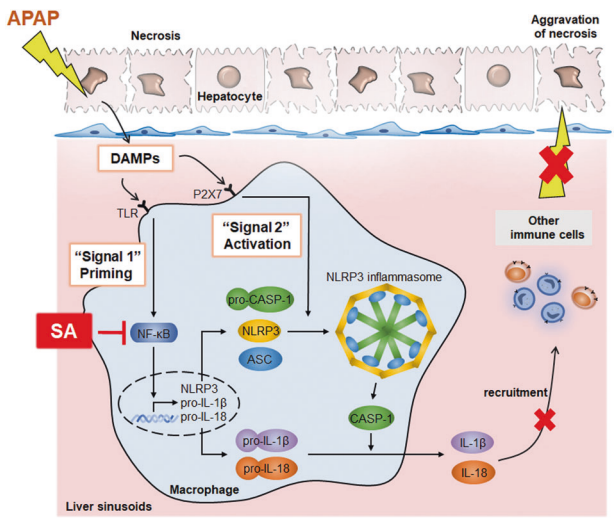

Fig. 6 SA treats AILI by inhibiting NLRP3 inflammasome activation in macrophages. APAP causes hepatocyte necrosis, which releases DAMPs and induces NLRP3-inflammasome-mediated macrophage pyroptosis. This leads to the secretion of pro-inflammatory factors, such as IL-1β and IL-18, that further recruits immune cells and aggravates liver inflammation, as well as hepatocyte damage. SA acts as an inhibitor of NF-κB signaling, NLRP3 inflammasome activation, and pyroptosis in macrophages, thereby reducing inflammation and protecting against AILI

The immune response is a key element of the immune defense system mediated by immune cells, and it plays an important role in eliminating necrotic cells and tissue debris [16, 17]. However, it also increases cellular damage in the late stage of AILI via mechanisms that are poorly understood. So far, only three types of anti-inflammatory drugs for AILI have been developed: DAMP inhibitors [57, 58], receptor antagonists [59–61] and immune cell

scavengers [47, 62, 63]. To be effective, these drugs must be administered within a short time after APAP ingestion. For example, the endogenous lipid mediator resolvin D2 (RvD2) can alleviate AILI by inhibiting neutrophils only if it is administered within 12 h of APAP ingestion [64]. The administration of RvD2 after 24 h of APAP administration is unfavorable for the regeneration of the late phase of AILI [64]. Considering the dual pro-inflammatory and anti-inflammatory effects of immune cells, the role of immune response in AILI remains highly controversial [47, 65].

In this study, we showed that SA inhibits NLRP3-inflammasome-mediated pyroptosis in macrophages by suppressing NF-κB signaling and the priming phase of NLRP3 inflammasome activation. This alleviates the hepatocyte damage caused by APAP both in vitro and in vivo. Moreover, the infiltration of neutrophils, dendritic cells, and $CD4^+$ T cells in AILI mice decreases after SA treatment. Overall, the results confirmed that SA affects the immune responses mediated by macrophages in the AILI model. However, further studies are needed to assess the effect of this compound on other immune cells.

Based on our findings, the immune response in AILI exhibits both pro-inflammatory and anti-inflammatory activity. When injury is inflicted by an ultra-high dose of APAP and the inflammation caused by immune cells exceeds a certain threshold, a large number of pro-inflammatory cytokines is released, which further aggravates the death of liver parenchymal cells. However, when the number of immune cells is relatively low and the immune response is weaker than that required for treatment, no pro-inflammatory or anti-inflammatory activities occur. In this case, the immune cells fail to promote the repair and regeneration of liver parenchymal cells in the late stage. Liver parenchymal cell repair can only be achieved when an appropriate number of immune cells are recruited in the late stage of AILI to secrete anti-inflammatory cytokines.

Our results also revealed that SA can be used as a supplementary agent with the only drug approved for AILI treatment (NAC). In the early stage of AILI, this drug protects liver parenchymal cells from damage by providing glutathione. However, its therapeutic window is narrow, as it has no effect in the late inflammatory stage of AILI. Recent studies show that by combining NAC with the neutrophil elastase inhibitor sivelestat, the expression of inflammatory markers and the number of monocytes in AILI mice can be reduced [66]. The efficacy of the combined treatment far exceeds that of NAC monotherapy [66], which suggests that combination drug intervention has broad prospects in AILI treatment. SA can also be combined with the NAC drug for AILI treatment; however, further research is needed to assess the effect of the combined therapy.

In conclusion, SA, a new type of sesquiterpene lactone compound extracted from *Baccaurea ramiflora* Lour., significantly inhibits the expression and activation of the NLRP3 inflammasome and pyroptosis in macrophages. It also protects macrophages from the pyroptosis caused by APAP-damaged liver cells, and SA-treated macrophages reduce the secondary death of liver cells. Furthermore, SA significantly alleviates AILI in mice by blocking inflammation and inhibiting the activation of NLRP3 inflammasomes. Overall, our findings reveal a previously unidentified role of SA in inhibiting NLRP3 inflammasome activation in macrophages and protecting liver cells from AILI, which suggests that this natural compound can be used to treat AILI.

ACKNOWLEDGEMENTS

We thank Prof. Lishe Gan for gifted Sapidolide A. This work was supported by the National Natural Science Foundation (Nos. 81903708, 82003873), the Zhejiang Provincial Natural Science Foundation (Nos. LR21H310001, LGF20H030001).

AUTHOR CONTRIBUTIONS

JJW and QJW designed and interpreted experiments. JCW, QS, and QZ performed experiments. DYL and LQZ contributed to the data acquisition. LLZ and YPQ analyzed data. BY and QJH critically reviewed the manuscript. JCW, QS, LLZ, and JJW wrote the paper.

ADDITIONAL INFORMATION

Supplementary information The online version contains supplementary material available at https://doi.org/10.1038/s41401-021-00842-x.

Competing interests: The authors declare no competing interests.

REFERENCES

1. Katarey D, Verma S. Drug-induced liver injury. Clin Med. 2016;16:s104–s9.
2. Fisher K, Vuppalanchi R, Saxena R. Drug-induced liver injury. Arch Pathol Lab Med. 2015;139:876–87.
3. Lee WM. Drug-induced acute liver failure. Clin Liver Dis. 2013;17:575–86. viii
4. Woolbright BL, Jaeschke H. Role of the inflammasome in acetaminophen-induced liver injury and acute liver failure. J Hepatol. 2017;66:836–48.
5. Ramachandran A, Jaeschke H. Acetaminophen hepatotoxicity. Semin Liver Dis. 2019;39:221–34.
6. Yang R, Tonnesseen TI. DAMPs and sterile inflammation in drug hepatotoxicity. Hepatol Int. 2019;13:42–50.
7. Jaeschke H, Ramachandran A. Mechanisms and pathophysiological significance of sterile inflammation during acetaminophen hepatotoxicity. Food Chem Toxicol. 2020;138:111240.
8. Fisher ES, Curry SC. Evaluation and treatment of acetaminophen toxicity. Adv Pharmacol. 2019;85:263–72.
9. Chiew AL, Gluud C, Brok J, Buckley NA. Interventions for paracetamol (acetaminophen) overdose. Cochrane Database Syst Rev. 2018;2:CD003328.
10. Hendrickson RG. What is the most appropriate dose of N-acetylcysteine after massive acetaminophen overdose? Clin Toxicol. 2019;57:686–91.
11. Kubes P, Jenne C. Immune responses in the liver. Annu Rev Immunol. 2018;36:247–77.
12. Knolle PA, Gerken G. Local control of the immune response in the liver. Immunol Rev. 2000;174:21–34.
13. Lewis PS, Campana L, Aleksieva N, Cartwright JA, Mackinnon A, O'Duibhir E, et al. Alternatively activated macrophages promote resolution of necrosis following acute liver injury. J Hepatol. 2020;73:349–60.
14. Yang W, Tao Y, Wu Y, Zhao X, Ye W, Zhao D, et al. Neutrophils promote the development of reparative macrophages mediated by ROS to orchestrate liver repair. Nat Commun. 2019;10:1076.
15. McGill MR, Sharpe MR, Williams CD, Taha M, Curry SC, Jaeschke H. The mechanism underlying acetaminophen-induced hepatotoxicity in humans and mice involves mitochondrial damage and nuclear DNA fragmentation. J Clin Invest. 2012;122:1574–83.
16. Cover C, Liu J, Farhood A, Malle E, Waalkes MP, Bajt ML, et al. Pathophysiological role of the acute inflammatory response during acetaminophen hepatotoxicity. Toxicol Appl Pharmacol. 2006;216:98–107.
17. Woolbright BL, Jaeschke H. Mechanisms of inflammatory liver injury and drug-induced hepatotoxicity. Curr Pharmacol Rep. 2018;4:346–57.
18. Sica A, Erreni M, Allavena P, Porta C. Macrophage polarization in pathology. Cell Mol Life Sci. 2015;72:4111–26.
19. Li M, Sun X, Zhao J, Xia L, Li J, Xu M, et al. CCL5 deficiency promotes liver repair by improving inflammation resolution and liver regeneration through M2 macrophage polarization. Cell Mol Immunol. 2020;17:753–64.
20. Wang Y, Zhao Y, Wang Z, Sun R, Zou B, Li R, et al. Peroxiredoxin 3 inhibits acetaminophen-induced liver pyroptosis through the regulation of mitochondrial ROS. Front Immunol. 2021;12:652782.
21. Miao EA, Rajan JV, Aderem A. Caspase-1-induced pyroptotic cell death. Immunol Rev. 2011;243:206–14.
22. Szabo G, Petrasek J. Inflammasome activation and function in liver disease. Nat Rev Gastroenterol Hepatol. 2015;12:387–400.
23. Imaeda AB, Watanabe A, Sohail MA, Mahmood S, Mohamadnejad M, Sutterwala FS, et al. Acetaminophen-induced hepatotoxicity in mice is dependent on Tlr9 and the Nalp3 inflammasome. J Clin Invest. 2009;119:305–14.
24. Williams CD, Antoine DJ, Shaw PJ, Benson C, Farhood A, Williams DP, et al. Role of the Nalp3 inflammasome in acetaminophen-induced sterile inflammation and liver injury. Toxicol Appl Pharmacol. 2011;252:289–97.
25. Williams CD, Farhood A, Jaeschke H. Role of caspase-1 and interleukin-1beta in acetaminophen-induced hepatic inflammation and liver injury. Toxicol Appl Pharmacol. 2010;247:169–78.

26. Du YC, Lai L, Zhang H, Zhong FR, Cheng HL, Qian BL, et al. Kaempferol from Penthorum chinense Pursh suppresses HMGB1/TLR4/NF-kappaB signaling and NLRP3 inflammasome activation in acetaminophen-induced hepatotoxicity. Food Funct. 2020;11:7925–34.
27. Cai C, Huang H, Whelan S, Liu L, Kautza B, Luciano J, et al. Benzyl alcohol attenuates acetaminophen-induced acute liver injury in a Toll-like receptor-4-dependent pattern in mice. Hepatology. 2014;60:990–1002.
28. Barman PK, Mukherjee R, Prusty BK, Suklabaidya S, Senapati S, Ravindran B. Chitohexaose protects against acetaminophen-induced hepatotoxicity in mice. Cell Death Dis. 2016;7:e2224.
29. Nesa ML, Karim SMS, Api K, Sarker MMR, Islam MM, Kabir A, et al. Screening of Baccaurea ramiflora (Lour.) extracts for cytotoxic, analgesic, anti-inflammatory, neuropharmacological and antidiarrheal activities. BMC Complement Alter Med. 2018;18:35.
30. Usha T, Middha SK, Bhattacharya M, Lokesh P, Goyal AK. Rosmarinic acid, a new polyphenol from baccaurea ramiflora lour. leaf: a probable compound for its anti-inflammatory activity. Antioxidants. 2014;3:830–42.
31. Pan ZH, Ning DS, Huang SS, Wu YF, Ding T, Luo L. A new picrotoxane sesquiterpene from the berries of Baccaurea ramiflora with antifungal activity against Colletotrichum gloeosporioides. Nat Prod Res. 2015;29:1323–7.
32. Luo P, Peng S, Yan Y, Ji P, Xu J. IL-37 inhibits M1-like macrophage activation to ameliorate temporomandibular joint inflammation through the NLRP3 pathway. Rheumatology. 2020;59:3070–80.
33. Swanson KV, Deng M, Ting JP. The NLRP3 inflammasome: molecular activation and regulation to therapeutics. Nat Rev Immunol. 2019;19:477–89.
34. He Y, Hara H, Nunez G. Mechanism and regulation of NLRP3 inflammasome activation. Trends Biochem Sci. 2016;41:1012–21.
35. Bauernfeind FG, Horvath G, Stutz A, Alnemri ES, MacDonald K, Speert D, et al. Cutting edge: NF-kappaB activating pattern recognition and cytokine receptors license NLRP3 inflammasome activation by regulating NLRP3 expression. J Immunol. 2009;183:787–91.
36. Franchi L, Eigenbrod T, Núñez G. Cutting edge: TNF-α mediates sensitization to ATP and silica via the NLRP3 inflammasome in the absence of microbial stimulation. J Immunol. 2009;183:792–6.
37. Lin KM, Hu W, Troutman TD, Jennings M, Brewer T, Li X, et al. IRAK-1 bypasses priming and directly links TLRs to rapid NLRP3 inflammasome activation. Proc Natl Acad Sci USA. 2014;111:775–80.
38. Xing Y, Yao X, Li H, Xue G, Guo Q, Yang G, et al. Cutting edge: TRAF6 mediates TLR/IL-1R signaling-induced nontranscriptional priming of the NLRP3 inflammasome. J Immunol. 2017;199:1561–6.
39. de Alba E. Structure, interactions and self-assembly of ASC-dependent inflammasomes. Arch Biochem Biophys. 2019;670:15–31.
40. Martinon F, Burns K, Tschopp J. The inflammasome: a molecular platform triggering activation of inflammatory caspases and processing of proIL-beta. Mol Cell. 2002;10:417–26.
41. Wang L, Manji GA, Grenier JM, Al-Garawi A, Merriam S, Lora JM, et al. PYPAF7, a novel PYRIN-containing Apaf1-like protein that regulates activation of NF-kappa B and caspase-1-dependent cytokine processing. J Biol Chem. 2002;277:29874–80.
42. Gunawan BK, Liu ZX, Han D, Hanawa N, Gaarde WA, Kaplowitz N. c-Jun N-terminal kinase plays a major role in murine acetaminophen hepatotoxicity. Gastroenterology. 2006;131:165–78.
43. Hanawa N, Shinohara M, Saberi B, Gaarde WA, Han D, Kaplowitz N. Role of JNK translocation to mitochondria leading to inhibition of mitochondria bioenergetics in acetaminophen-induced liver injury. J Biol Chem. 2008;283:13565–77.
44. Mihm S. Danger-associated molecular patterns (DAMPs): molecular triggers for sterile inflammation in the liver. Int J Mol Sci. 2018;19:3104.
45. Martin-Murphy BV, Holt MP, Ju C. The role of damage associated molecular pattern molecules in acetaminophen-induced liver injury in mice. Toxicol Lett. 2010;192:387–94.
46. Yang H, Antoine DJ, Andersson U, Tracey KJ. The many faces of HMGB1: molecular structure-functional activity in inflammation, apoptosis, and chemotaxis. J Leukoc Biol. 2013;93:865–73.
47. Liu ZX, Govindarajan S, Kaplowitz N. Innate immune system plays a critical role in determining the progression and severity of acetaminophen hepatotoxicity. Gastroenterology. 2004;127:1760–74.
48. Dixon LJ, Barnes M, Tang H, Pritchard MT, Nagy LE. Kupffer cells in the liver. Compr Physiol. 2013;3:785–97.
49. Mossanen JC, Krenkel O, Ergen C, Govaere O, Liepelt A, Puengel T, et al. Chemokine (C-C motif) receptor 2-positive monocytes aggravate the early phase of acetaminophen-induced acute liver injury. Hepatology. 2016;64:1667–82.
50. Zigmond E, Samia-Grinberg S, Pasmanik-Chor M, Brazowski E, Shibolet O, Halpern Z, et al. Infiltrating monocyte-derived macrophages and resident kupffer cells display different ontogeny and functions in acute liver injury. J Immunol. 2014;193:344–53.
51. Zhang C, Feng J, Du J, Zhuo Z, Yang S, Zhang W, et al. Macrophage-derived IL-1alpha promotes sterile inflammation in a mouse model of acetaminophen hepatotoxicity. Cell Mol Immunol. 2018;15:973–82.
52. Gehrke N, Hovelmeyer N, Waisman A, Straub BK, Weinmann-Menke J, Worns MA, et al. Hepatocyte-specific deletion of IL1-RI attenuates liver injury by blocking IL-1 driven autoinflammation. J Hepatol. 2018;68:986–95.
53. Dias DA, Urban S, Roessner U. A historical overview of natural products in drug discovery. Metabolites. 2012;2:303–36.
54. Kim BM. The role of saikosaponins in therapeutic strategies for age-related diseases. Oxid Med Cell Longev. 2018;2018:8275256.
55. Atanasov AG, Waltenberger B, Pferschy-Wenzig EM, Linder T, Wawrosch C, Uhrin P, et al. Discovery and resupply of pharmacologically active plant-derived natural products: a review. Biotechnol Adv. 2015;33:1582–614.
56. Subramanya SB, Venkataraman B, Meeran MFN, Goyal SN, Patil CR, Ojha S. Therapeutic potential of plants and plant derived phytochemicals against acetaminophen-induced liver injury. Int J Mol Sci. 2018;19:3776.
57. Yan M, Huo Y, Yin S, Hu H. Mechanisms of acetaminophen-induced liver injury and its implications for therapeutic interventions. Redox Biol. 2018;17:274–83.
58. Yang H, Wang H, Ju Z, Ragab AA, Lundback P, Long W, et al. MD-2 is required for disulfide HMGB1-dependent TLR4 signaling. J Exp Med. 2015;212:5–14.
59. Salama M, Elgamal M, Abdelaziz A, Ellithy M, Magdy D, Ali L, et al. Toll-like receptor 4 blocker as potential therapy for acetaminophen-induced organ failure in mice. Exp Ther Med. 2015;10:241–6.
60. Ekong U, Zeng S, Dun H, Feirt N, Guo J, Ippagunta N, et al. Blockade of the receptor for advanced glycation end products attenuates acetaminophen-induced hepatotoxicity in mice. J Gastroenterol Hepatol. 2006;21:682–8.
61. Hoque R, Sohail MA, Salhanick S, Malik AF, Ghani A, Robson SC, et al. P2X7 receptor-mediated purinergic signaling promotes liver injury in acetaminophen hepatotoxicity in mice. Am J Physiol Gastrointest Liver Physiol. 2012;302:G1171–9.
62. Laskin DL, Gardner CR, Price VF, Jollow DJ. Modulation of macrophage functioning abrogates the acute hepatotoxicity of acetaminophen. Hepatology. 1995;21:1045–50.
63. Liu ZX, Han D, Gunawan B, Kaplowitz N. Neutrophil depletion protects against murine acetaminophen hepatotoxicity. Hepatology. 2006;43:1220–30.
64. Patel SJ, Luther J, Bohr S, Iracheta-Vellve A, Li M, King KR, et al. A novel resolvin-based strategy for limiting acetaminophen hepatotoxicity. Clin Transl Gastroenterol. 2016;7:e153.
65. Liaskou E, Wilson DV, Oo YH. Innate immune cells in liver inflammation. Mediators Inflamm. 2012;2012:949157.
66. Raevens S, Van Campenhout S, Debacker PJ, Lefere S, Verhelst X, Geerts A, et al. Combination of sivelestat and N-acetylcysteine alleviates the inflammatory response and exceeds standard treatment for acetaminophen-induced liver injury. J Leukoc Biol. 2020;107:341–55.